Multispectral Satellite Imagery Retrieval Based on Probabilistic Distance Measure

K. Seetharaman[1]
Department of Computer Science & Engineering
Annamalai University, Annamalainagar – 608 002,
Tamil Nadu, INDIA, email:kseethadde@yahoo.com

W. T. Chembian
Department of Computer Science & Engineering,
Jay Institute of Technology, Chennai – 631 204, Tamil Nadu, INDIA, email:wtchembian@gmail.com

Abstract— This paper proposes a novel method, based on a probabilistic distance measure, penalized Hellinger's distance. The proposed method converts the input color query image to the HSV color space. The texture and structure components of the query imagery are segregated and compared to the target imageries in the imagery database individually at a specific significance level. If both the texture and structure components pass the test at a significance level, then it is assumed that the query imagery belongs to the same or similar class of imageries. The target imageries are marked, indexed, and retrieved. Otherwise, it is assumed that the query imagery does not match with the imageries in the imagery database. The attained results reveal that the proposed probabilistic distance-based method yields better results.

Keywords— Probabilistic distance measure, Hellinger distance, multispectral imageries, target imagery, query imagery.

I. INTRODUCTION

In the last two decades the imagery mining turned the attention of many researchers in the Computer Vision domain. A number of researchers have developed a manifold method [1,2,3] related to CBIR, among them, the distance-based method plays a significant role in image retrieval. Liu et al. [1] propose a region-based image retrieval method with high-level semantics and decision trees. In [3], Markov random field-based similarity regions have been defined. They have been built using a self-complementary area filter that stems from the morphological theory. This filter splits up the original image into flat zones, where the underlying pixels have the same spectral values. Once the MRF has been clearly established, the abundances, a hierarchical Bayesian algorithm is employed to estimate the class labels, the noise variance, and the corresponding hyperparameters. Further, a hybrid Gibbs sampler is constructed to generate samples according to the corresponding posterior distribution of the unknown parameters and hyperparameters.

The relevance feedback model for content-based image retrieval using multiple similarity measures is introduced, which is independent from similarity measures, that is, probability-based retrieval [4,5]. Wang et al. [6] presents a texture feature-based color image retrieval, which uses the color co-occurrence matrix to extract the texture feature and measure the similarity of two color images. It also taken into consideration of the components and distribution, and the feature obtained reflects the texture correlation and represents the color information. They claim that their method is superior to the gray-level co-occurrence matrix method and color histogram method, and it enhances the retrieval accuracy. E. Walia and A. Pal [7] have introduced a framework for color image retrieval, which utilize the Angular Radial Transform and the modified Color Difference Histogram to extract color, texture, and shape information of images. Yang and Hao [8][1] developed a Color Layer-Based Texture Elements Histogram method, based on the combination of one group of texture elements and the quantized HSV color information. Further, they extract color features using Color Fuzzy Correlogram technique. Cerra and Datcu [9] developed a method for color image retrieval, which is fast compression-based similarity measures with dictionaries.

Scot et al, [10] perform content-based shape retrieval of objects from a large-scale satellite imagery database. The Objects of multiple scales are automatically extracted from satellite imagery and then encoded into a bitmap shape representation. This shape encoding compresses the total size of the shape descriptors to approximately 0.34% of the imagery database size. They have developed the entropy-balanced bitmap (EBB) tree, which exploits the probabilistic nature of bit values in automatically derived shape classes. The efficiency of the shape representation coupled with the EBB tree allows us to index approximately 1.3 million objects for fast content-based retrieval of objects by shape.

Grana and Veganzones [11] propose a CBIR system for hyper-spectral image retrieval with the help of spectral information, and end-member induction algorithm is adopted. Ozdemir and Karnieli [11] have proposed a method, which investigates the potential of using WordView-2 multispectral satellite imagery for predicting forest structural parameters in a dryland plantation forest in Israel. It extracts the relationships between the image texture features and the several structural parameters, such as Number of Trees (NT), Basal Area (BA), Stem Volume (SV), Clark-Evans Index (CEI), Diameter Differentiation Index (DDI), Contagion Index (CI), Gini Coefficient (GC), and Standard Deviation of Diameters at Breast Heights (SDDBH) were examined using correlation analyses. Also, it concludes that the cross-validated statistics confirmed that the structural parameters including the BA, SDDBH, and GC can be predicted and mapped with a reasonable accuracy using the texture features extracted from the spectral bands of the WorldView-2 image.

Im et al. [13] proposed a change detection method based on an object or neighbourhood correlation image analysis and image segmentation methods. The correlation image analysis takes account of pairs of brightness values from the geographic region or object between bi-temporal image datasets leads to

[1] Corresponding author.

be highly correlated when little change occurs, and uncorrelated while change occurs. They have also investigated five different change detection methods, such as object-based change classification incorporating object correlation images (OCIs), object-based change classification incorporating neighbourhood correlation images (NCIs), object-based change classification without contextual features, per-pixel change classification incorporating NCIs, and traditional per-pixel change classification using only bi-temporal image data, to determine how new contextual features could improve change classification results. As a result, they reported that Object-based change classifications incorporating the OCIs or the NCIs yields more accurate change detection classes than the other change detection results. Su et al. [14] proposed a geographically adaptive inversion model to better estimates of bottom depth. The model parameters are optimally determined within a geographical region, in contrast to the entire scene of the global inversion model. By using high-resolution IKONOS and moderate-resolution Landsat satellite imageries, they proved that regionally and locally calibrated inversion models can effectively address the problems introduced by spatial heterogeneity in water quality and bottom type, and provide significantly improved bathymetric estimates for more complex coastal waters. Yang and Newsam [15] have investigated local invariant features for geographic image retrieval for image retrieval of land-use/land-cover (LULC) classes in high-resolution aerial imagery, and suggested that the local invariant features are well suited for the aerial and satellite imageries. They also have reported that the effects of a number of design parameters on a bag-of-visual-words (BOVW) representation including saliency-versus grid-based local feature extraction, the size of the visual codebook, the clustering algorithm used to create the codebook, and the dissimilarity measure used to compare the BOVW representations. Furthermore, they have performed comparisons with the standard features, such as color and texture.

Swarnambiga and Vasuki [16] consider medical image retrieval system and apply various distance measures, such as the Euclidean, Manhattan, Mahalanobis, Bray Curtis, Canberra, Squared chord, and Chi-square; they compare these methods and suggest that the Euclidean distance measure yields better results than the others. Frery, et al. [17] introduced a stochastic distance measure, that is, revised Wishart and Bartlett distance measures which measure the distances between four relaxed scaled complex Wishart distributions. Based on these distances a new test statistic is derived, which leads asymptotic Chi-square distribution. They implemented the measure with the actual data, which illustrate the discrimination and homogeneity identification capabilities of these distances; and reported that the distance measure yields better results for segmentation and classification of images. Malik and Baharudine [18] introduce a technique, based on the similarity measures, such as Euclidean distance, City block distance, Canberra distance, maximum value distance, Minkowski distance, which are employed on the features extracted from the DC and AC coefficients of the compressed images.

Though a number of methods available for multispectral satellite imagery retrieval, the statistical methods such as test of hypothesis-based and statistical distance-based measures, play a noteworthy role in the domain of computer vision and multimedia, especially in imagery retrieval. The test of hypothesis-based methods are applied straightforward on the raw pixel intensity values while the statistical distance-based methods are employed on the features, such as color, texture, shape, spatial orientation of the pixels; and some other statistical features, i.e., mean, standard deviation, skewness, kurtosis, correlation, etc., extracted from the intensity values of the imagery.

Many of the distance-based methods, such as Batachariya distance, Kullback-Leibler, Mahalanabis distance, Chi-square distance are applied straight on the intensity values of the imagery. The review of literature explore that the distance-based methods are simple, effective, and efficient for imagery retrieval. With the consideration of these points, in this paper, the Penalized Hellingers Distance (PHD) [19] is adopted.

The rest of the paper is organized as follows. Section II describes the proposed retrieval method. Section III briefs the measure of performance. In section IV, experimental results have been illustrated, and a brief discussion about the comparative study about the performance and the computational time consumed by the proposed method and the existing methods have been discussed. Finally, Section V concludes the paper with a conclusion.

II. BASIS OF THE PROPOSED DISTANCE MEASURE

Let us assume that the query and target imageries are identically independently distributed to Gaussian random process; and the intensity values of the query and target imageries, represented by $Q = (q_1, q_2, ..., q_n)$ and $T = (t_1, t_2, ..., t_n)$ respectively. The Gaussian distribution of the query and target imageries can be denoted as $Q \sim N(\mu, \sigma^2)$ and $T \sim N(\mu, \sigma^2)$ respectively. The probability density function of the query imagery can be defined as

$$f(q_i: \mu_q, \sigma_q^2) = \frac{1}{\sigma_q \sqrt{2\pi}} exp\left(\frac{-(q_i - u_q)^2}{2\sigma_q^2} \right) \quad (1)$$

and the probability density function of the target imagery can be defined as

$$f(t_i: \mu_t, \sigma_t^2) = \frac{1}{\sigma_t \sqrt{2\pi}} exp\left(\frac{-(t_i - u_t)^2}{2\sigma_t^2} \right) \quad (2)$$

where, μ represents the spectrum of the intensity values of the imagery

$$\mu_q = \frac{\sum_{i=1}^{n} q_i}{n} \quad (3)$$

$$\mu_t = \frac{\sum_{i=1}^{n} t_i}{n} \quad \text{and} \quad (4)$$

$$\sigma_q^2 = \frac{\sum_{i=1}^{n} (q_i - \mu_q)^2}{n_q - 1} \quad (5)$$

$$\sigma_t^2 = \frac{\sum_{i=1}^{n} (t_i - \mu_t)^2}{n_t - 1} \quad (6)$$

A. Proposed Image Retrieval Distance Measure

As discussed in the previous section, the query and target imageries are assumed to be two discrete normal probability distributions, i.e. Q = (q_1, q_2, ..., q_n) and T = (t_1, t_2, ..., t_n), and the intensity values of the query imagery, q_i, and the target imagery, t_i, are treated as two different probability distributions. In 1909, Hellinger introduced a distance measure, which is modified and proposed by Kupperman in 1957; and the same distance measure is also modified by Salicru et al. [19] which is expressed in equation (7).

$$\mathrm{PHD} = 2\frac{m_1 m_2}{m_1 + m_2} D_{\varpi}\left(f_{\rho_1}, f_{\rho_2}\right) \tag{7}$$

where, m_1 and m_2 are the number of pixel values of the query and target imageries, respectively; $D_{\varpi}\left(f_{\rho_1}, f_{\rho_2}\right)$ is the ω-divergence or ω-disparity between $f\hat{\rho}_1$ and $f\hat{\rho}_2$ and the expression is presented in equation (8)

$$D_{\omega}\left(f_{\hat{\rho}_1}, f_{\hat{\rho}_2}\right) = \sum_{j=0}^{\infty} f_{\hat{\rho}2}(x_j)\omega\left(\frac{f_{\hat{\rho}1}\left(x_j\right)}{f_{\hat{\rho}2}\left(x_j\right)}\right), \omega \in \varpi^* \tag{8}$$

where, $\hat{\rho}_1$ and $\hat{\rho}_2$ are the maximum likelihood estimators of ρ_1 and ρ_2; $f\hat{\rho}_2(x_j)$ is the distribution function of the imagery x_j : j = Q, T; where, ω* is the class of all convex functions ω(x), x ≥ 0.

The joint likelihood function, based on the query imagery q_1, …, q_{m1} and the target imagery t_1, …, t_{m1}, is given by

$$L\left(\rho_1, \rho_2\right) = \prod_{j=0}^{\infty} f_{\rho_1}\left(q_j\right)^{n_1(q_j)} f_{\rho_2}\left(t_j\right)^{n_2(t_j)} \tag{9}$$

and if we denote by $\tilde{\rho}$ the maximum likelihood estimates of the common parameter under the hypothesis $\rho_1 = \rho_2$ the log likelihood ratio test statistic is given by

$$\mathrm{LRT} = 2\left[\log L\left(\hat{\rho}_1, \hat{\rho}_2\right) - \log L\left(\hat{\rho}, \hat{\rho}\right)\right] \tag{10}$$

which is asymptotically distributed to a Chi-square distribution. In order to match the query and target imageries, the hypothesis is framed below. The hypothesis is framed to test the statistic expressed in equation (7), based on the mean values, i.e., spectrum of the energy of the intensity values.

Hypothesis:

$$H_o: \mu_q = \mu_t \text{ (similarity)}$$
$$H_1: \mu_q \neq \mu_t \text{ (disimilarity)}$$

***Critical Region*:** Since the PHD statistic value is asymptotically distributed to Chi-square (χ^2) distribution, the PHD is compared to the critical value of the χ^2_{α} in the statistical table with degrees of freedom $(n_q + n_t - 1)$, where α is the level of significance. If $\mathrm{PHD} < \chi^2_{\alpha}$ at the level of significance α, then it is inferred that the query and target imageries are same or similar (i.e., belong to the same class); otherwise, the two imageries differ (i.e. belong to different classes). Based on the distance values, the imageries are marked and indexed in ascending order, and the indexed imageries are retrieved.

III. MEASURE OF PERFORMANCE

Though, there are many performance measures, this paper considers the Average Normalized Modified Retrieval Rank (ANMRR) measure, because it is a single measure of performance, which considers both the number and order of the ground truth items that appear in the top retrievals [15]. The ANMRR score computed to measure the performance of the proposed method for a set, N_S, of the query images. The ANMRR and its derivatives have been expressed in Eqs. (11), (12), (13), and (14). Also, the performance of the proposed method was measured in terms of precision (P) [20] for the same set of images, which is expressed in Eq. (15), and compared with the state-of-the-art methods.

$$\mathrm{ANMRR} = \frac{1}{N_s}\sum_{q=1}^{N_q} \mathrm{NMRR}(q) \tag{11}$$

The ANMRR value ranges from zero to one; the lower values indicate better retrieval rate. The normalized modified retrieval ranking (NMRR) score is defined in Eq. (12).

$$\mathrm{NMRR}(q) = \frac{\mathrm{AVR}(q) - 0.5\left(1 + N_q\right)}{1.25K_q - 0.5\left(1 + N_q\right)} \tag{12}$$

The NMRR(q) takes values between zero (whole ground truth found) and one (nothing found) irrespective of the size of the ground-truth for query image, q, NG(q). Finally, the ANMRR can be computed for a set NQ of the queries.

The NMRR score eliminates the influences of different Nq, which represents a set of query images. The average rank (AVR) for a single query is computed as

$$\mathrm{AVR}(q) = \frac{1}{N_s}\sum_{k=1}^{N_q} \mathrm{Rank}(k) \tag{13}$$

$$\mathrm{Rank}(q) = \begin{cases} \mathrm{Rank}(k), & \text{if Rank}(k) \leq K(q) \\ 1.25K(q), & \text{if Rank}(k) > k(q) \end{cases} \tag{14}$$

$$P = \frac{\left|\{\text{Relevant Images}\} \cap \{\text{Retrieved Images}\}\right|}{\left|\text{Retrieved Images}\right|} \tag{15}$$

The Rank(k) of the k-th item is defined as a position at which it is retrieved. An item with higher rank was given a constant penalty, if a number $K_q \geq N_q$ was chosen. The K_q is generally chosen to be 2Nq.

IV. EXPERIMENTAL RESULTS

To validate the proposed distance measure, more than 1200 multispectral satellite imageries were collected from various sources through the Internet, and subjected to the experiment. For a sample, some of them have been presented in this paper. A satellite colour imagery is given as input key to the system. The inputted key imagery is modeled to HSV colour space. The texture and structure components are segregated, based on the V components. For a sample, the segregated texture and

structure components of the input key imagery have been presented in Figure 1.

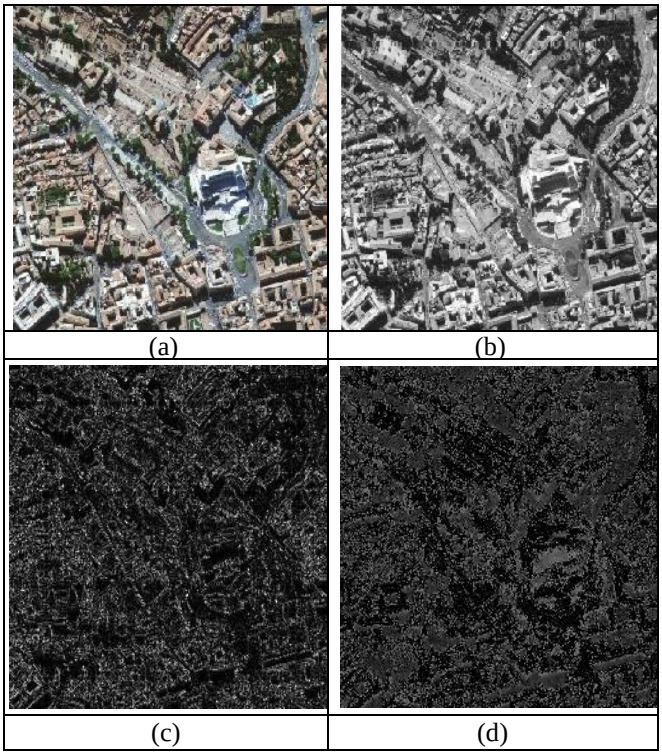

Figure 1: (a): actual imagery; (b): gray-scale imagery; (c): structure component of (b); (d): texture component of (b).

The penalized Hellinger's divergence measure, $D(f\hat{\rho}_1, f\hat{\rho}_2)$ is computed, based on the expression in equation (7), for the input query imagery. The query and target imageries are considered in various combinations, and the computed $D(f\hat{\rho}_1, f\hat{\rho}_2)$ values are tested using the Chi-square distribution. In order to validate the proposed system, the imagery in Figure 2(a) is given as an input query to the system, for which the system retrieves the imageries in Figure 2(b). The retrieved output imageries show that the proposed Hellinger's divergence measure is robust for scaling and rotation. Because of the proposed distance measure is distribution-based, it is invariant for scaling, rotation, and noise. The experiment is conducted at various levels of significance to the input query imagery given in Figure 2(a). The imageries in column 2 of the Figure 2(b) are retrieved at 5% level of significance; imageries in columns 3, 2, and 1 are retrieved at 10% level of significance; while fixing significance level at 15%, the system retrieves the imageries in columns 4, 3, 2, and 1; and all the imageries were retrieved at the level of significance, 20%.

(a)

(b)

Figure 2. (a): actual query imagery; (b): retrieved target imageries.

The main advantage of the proposed system is that it facilitates the user to retrieve only the required number of imageries by fixing the level of significance at a specified level, whereas the existing methods retrieve a number of similar imageries. Thus, in the existing methods, the user has to expend the time to select required imageries from the set of retrieved same or similar imageries. In addition to that the proposed system retrieves a set of similar imageries by fixing the levelof significance at a desired level.

Moreover, to emphasize the efficiency of the proposed system, a number of textured, semi-structured, and structured images considered from the CalTech and Holidays image database; and the obtained retrieved images have been presented in Figure 3. The system retrieved the images in columns 2–6 for the input query images in column 1. The images in in column 2 were retrieved at the level of significance, 0.01 (i.e. 1%); the images in column 3 were retrieved while the level of significance is fixed at 0.06 or lesser (i.e. 6% or lesser); while the level of significance was fixed at 0.12 or lesser (i.e. 12% or lesser), the images in columns 4 and 5 were retrieved; images in column 6 were retrieved at the level of significance, 0.16 (i.e. 16% or lesser).

ISSN: 2393-9028 (PRINT) | ISSN: 2348-2281 (ONLINE)

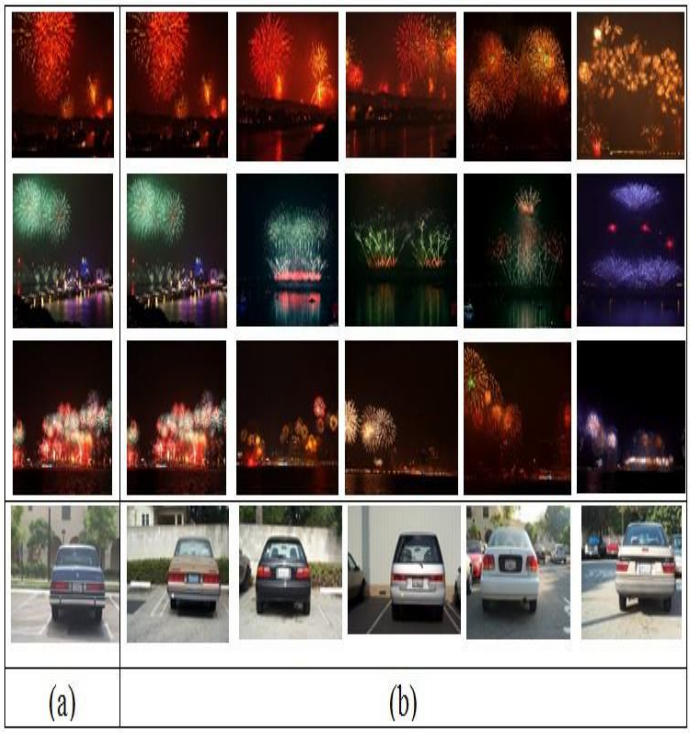

Figure 3: CalTech and Holidays Images Texture or Semi-structured imageries. Column1: input query imageries; columns 2-6: retrieved output imageries.

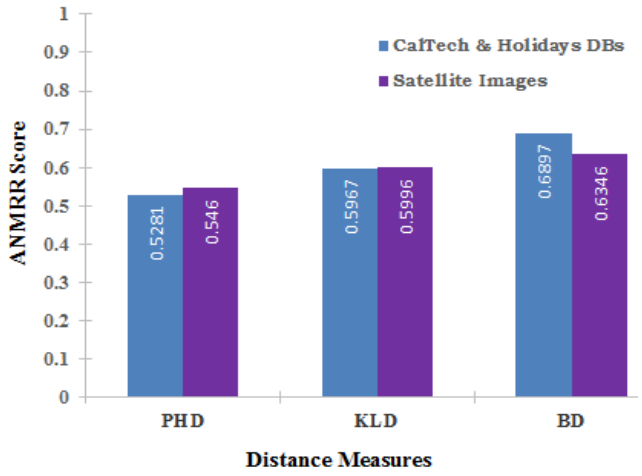

Figure 4. Comparison PHD with KLD and BD.

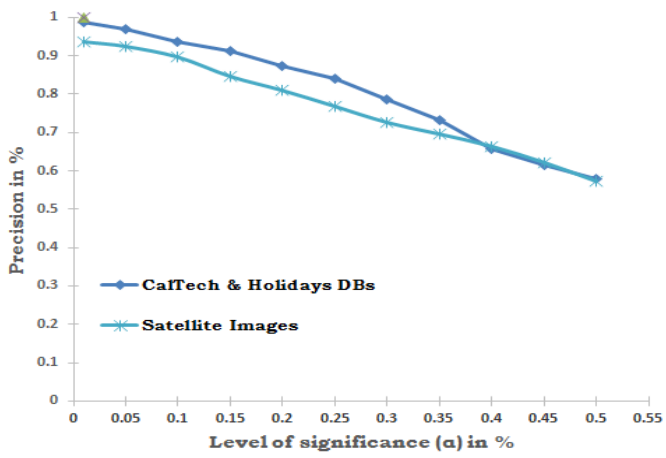

Figure 5. Performance of the proposed method in terms of precision versus recall.

A comparative study was performed, in order to measure the efficiency of the proposed method, with the existing methods: Bhatacharyya distance (BD) [15] and Kullback-Leibler distance (KLD) [21], in terms of Average Normalized Modified Retrieval Rank (ANMRR) score and average precision (AP) values of the retrieved results. The average of the precision values is obtained at the level of significance (α) 0.15 percent. The obtained results reveal that the proposed method outperforms the existing systems. The AP and ANMRR scores were calculated for the proposed system and the existing methods, KLD and BD, and the obtained results have been presented in Table 1. A diagrammatic representation of the comparative study of the proposed method with the KLD and BD measures is given in Figure 4. Also, a line graph was sketched for the precision values attained at various significance levels, and it has been shown in Figure 5.

TABLE I. PERFORMANCE OF THE PROPOSED SYSTEM WITH EXISTING METHODS.

Image Database	Proposed Method		KLD Method		BD Method	
	AP	ANMRR	AP	ANMRR	AP	ANMRR
CalTech & Holidays	0.8078	0.5281	0.7293	0.5781	0.7037	0.5963
Satellite Images	0.7692	0.546	0.6991	0.5896	0.6863	0.6068

A. *Time Complexity*

The performance of the proposed system was compared with the existing systems: KLD and BD distance measures in terms of computational time complexity. The system was implemented using Java SE 7 compiler with the system specification, Intel Core i5-4440 processor-based PC with 4GB DDR3 RAM. The time consumed by the proposed system for feature extraction, matching and retrieving the imageries was measured in terms of seconds after a rigorous experimentation, and the obtained results were presented in Table 2. The proposed system demands lesser time compared to that of the existing systems, and also the proposed system yields better retrieval results.

TABLE II. COMPARISON OF COMPUTATIONAL TIME COMPLEXITY.

Time Consumption	Proposed System	KLD	BD
Feature Extraction Time	0.485 sec	0.975 sec	0.852 sec
Searching Time	0.058 sec	0.070 sec	0.069 sec

V. CONCLUSION

The given input query image is segregated into texture and structure components, and they compared to the target images in the image database by performing the tests of hypothesis, based on the Hellinger's distance measure, at a specific significant level (α). If both the texture and structure components of the query image pass the test at the significant

level, then it was inferred that the query and target images belong to same class; otherwise, it is assumed that they belong to different classes. Furthermore, texture, structure, and semi-structured images were subjected to the experiment, for which, the proposed system performs well comparatively better than the existing methods.

REFERENCES

[1] Liu, Y., Zhang, D., Lu, G., (2008). Region-based image retrieval with high-level semantics using decision tree learning, Pattern Recognition, vol. 41, 2554 – 2570.

[2] Zhang, D.,Tang, J., Jin, G., Zhang, Y., Tian, Q. 2018. Region similarity arrangement for large-scale image retrieval, Neurocomputing, vol. 272, p. 461–470

[3] Eches, O., Benediktsson, J. A., Dobigeon, N., Tourneret, J-Y., 2013. Adaptive Markov Random Fields for Joint Unmixing and Segmentation of Hyperspectral Images, IEEE Transactions on Image Processing, vOL. 22(1), pp. 5-16.

[4] Seetharaman, K., 2015. Image retrieval based on micro-level spatial structure features and content analysis using Full Range Gaussian Markov Random Field model, Engineering Applications of Artificial Intelligence, vol, 40, pp. 103-116.

[5] Seetharaman, K., Jaikarthic, M., 2014. Statistical Distributional Approach for Scale and Rotation Invariant Colour Image Retrieval Using Multivariate Parametric tests and Orthogonality Condition, Journal of Visual Communication and Image Representation, vol. 25(5), pp. 727-739.

[6] X. Wang, Z.Chen, J. Yun, 2012. An effective method for color image retrieval based on texture, Computer Standards & Interfaces, vol. 34(1), pp. 31–35.

[7] E. Walia, A. Pal. Fusion framework for effective color image retrieval. Journal Visual Communication and Image Representation 2014, 25, 1335–1348.

[8] F. Yang and M. Hao, Effective Image Retrieval Using Texture Elements and Color Fuzzy Correlogram. Information, 2017, vol. 8(27), pp. 1-11.

[9] Cerra, D., Datcu, M., (2012). A Fast Compression-based Similarity Measure with Applications to Content-based Image Retrieval, Journal of Visual Communication and Image Representation, vol. 23(2), pp. 293–302.

[10] Scott, G.J., Klaric, M. N., Davis, C.H., Shyu, C-R., 2011. Entropy-Balanced Bitmap Tree for Shape-Based Object Retrieval From Large-Scale Satellite Imagery Databases, IEEE Transactions On Geoscience And Remote Sensing, vol. 49(5), pp. 1603-1616.

[11] Grana and Veganzones, M. A., (2012). An endmember-based distance for content based hyperspectral image retrieval, Pattern Recognition, vol. 45, pp. 3472–3489.

[12] Ozdemir, I., Karnieli, A. 2011. Predicting forest structural parameters using the image texture derived from WorldView-2 multispectral imagery in a dryland forest, Israel, International Journal of Applied Earth Observation and Geoinformation, vol. 13, pp. 701–710.

[13] Im, J., Jensen, J. R., Tullis, J. A., 2008. Object-based change detection using correlation image analysis and image segmentation. International Journal of Remote Sensing, vol. 29(2), pp. 399–423.

[14] Su, H., Liu, H., Wang, L., Filippi, A. M., Heyman, W. D., Beck, R. A., 2014. Geographically Adaptive Inversion Model for Improving Bathymetric Retrieval From Satellite Multispectral Imagery. IEEE Transactions on Geoscience and Remote Sensing, vol. 52(1), pp. 465 – 476.

[15] Yang, Y., and Newsam, S., Geographic Image Retrieval Using Local Invariant Features, IEEE Transaction on Geoscience and remote Sensing, vol. 51(2), 2013, pp. 878 – 832.

[16] Swarnambiga, A.,Vasuki, M. (2013). Medical Image Retrieval using Transforms, Applied Medical Informatics,vol. 32(2), pp: 54-66.

[17] Frery, A. C., Nascimento, A. D. C., and Cintra, R. J., 2014. Analytic Expressions for Stochastic Distances Between Relaxed Complex Wishart Distributions. IEEE Transactions on Geoscience and Remote Sensing, vol. 52(2), pp. 1213 – 1226.

[18] Malik, F., Baharudin, B., Analysis of distance metrics in content-based image retrieval using statistical quantized histogram texture features in the DCT domain, Journal of King Saud University – Computer and Information Sciences (2013) 25, 207–218.

[19] Salicrú, M., Morales, D., Menéndez, M.L., Pardo, L., 1994. On the applications of divergence type measures in testing statistical hypotheses. Journal of Multivariate Analysis, vol. 51, pp. 372–391.

[20] Powers, D.M.W., 2011. Evaluation: From Precision, Recall and F-Measure to ROC, Informedness, Markedness and Correlation, Journal of Machine Learning Technologies, Volume 2(1), pp-37-63.

[21] Sumana, I.J., Lu, G., and Zhang, D., 2012. Comparison of Curvelet and Wavelet Texture Features for Content Based Image Retrieval, IEEE International Conference on Multimedia and Expo, pp. 290-295. DOI 10.1109/ICME.2012.90.